Decay of oriented Rydberg wave packets excited with far-infrared radiation

G. M. Lankhuijzen,[1] M. Drabbels,[1] F. Robicheaux,[2] and L. D. Noordam[1]
[1]*FOM Institute for Atomic and Molecular Physics, Kruislaan 407, 1098 SJ Amsterdam, The Netherlands*
[2]*Department of Physics, 206 Allison Laboratory, Auburn University, Alabama 36849-5311*
(Received 29 July 1997)

Transitions from bound atomic Rydberg Stark states in a static electric field to autoionizing Rydberg states above the electric-field-induced ionization threshold are studied using a broadband, tunable free-electron laser (photon energy 160–1400 cm^{-1}, pulse duration ~ 1 ps) and compared with multichannel quantum defect theory calculations. An atomic streak camera is used to record the time-resolved electron emission transients of the autoionizing atoms. For Stark states located on the downfield side of the potential, the far-infrared ionization spectrum is found to be smooth and the electron emission prompt (<2 ps), whereas for Stark states located on the upfield side, the far-infrared spectrum has sharp resonances, and the lifetime of the quasicontinuum states is considerably longer. The electron-emission transients from optical ionization of ground-state atoms are compared to transients from far-infrared ionization of Rydberg atoms, showing that the angular motion of the wave packet is responsible for the ionization dynamics for both cases, but different coherent superpositions of angular momentum states are excited depending on the initial state. Finally, we discuss the feasability of using Rydberg atoms as an ultrafast far-infrared detector, starting from a downfield state, or as a wavelength-selective detector, starting from an upfield state. [S1050-2947(98)03601-4]

PACS number(s): 32.60.+i, 32.80.Rm, 33.30.Bv

I. INTRODUCTION

The structure and dynamics of highly excited electrons in atoms have been investigated using optical techniques in both the frequency and time domains. In the frequency domain, spectroscopic techniques have given detailed insight into the structure of the electronic states [1,2], while the use of short optical pulses enables the study of the dynamics of the highly excited electrons in the time domain [3–5]. The evolution of the resulting wave packet starts from the region of the initial state. In most experiments, the optical excitation started from the ground state or at least from an electronic state that was still confined to the core region. Hence for these wave packets the core was the starting point, e.g., [4,6,7]. If the *initial* state is prepared to be a Rydberg state instead of a ground state, the starting point of the electron is no longer confined to the core region and interesting new phenomena arise. For instance, if we place the Rydberg atom in a static electric field, the Rydberg atom will have a fixed dipole moment. We can therefore create wave packets starting from a Rydberg state that have a different localization with respect to the atomic core. The electron can be localized on either the downfield side or the upfield side of the nucleus. Creating a coherent superposition of high-lying Rydberg states starting from such an initial Rydberg state has been experimentally frustrated since the wavelength of the radiation required to make these transitions lies in the far-infrared regime. Only long pulse [8] and blackbody [9] radiation have been used to study these transitions. Note that at even longer (submillimeter) wavelengths THz half-cycle pulses are used to study the ionization behavior of oriented Rydberg wave packets [10,11].

Here we report wave-packet excitations using a free-electron laser, which operates in the photon-energy regime from 100 to 1600 cm^{-1}, enabling the study of the excitation from these bound, oriented Rydberg states to higher-lying autoionizing Rydberg states. The short pulse nature of the free-electron laser ($\tau_{\mathrm{pulse}} \sim 1$ ps) enables us also to study the dynamics of far-infrared excited Rydberg states in an electric field. The lifetime of the quasicontinuum states, i.e., states that have an energy higher than the field-induced ionization threshold, has been studied both experimentally [12–15] and theoretically [16,17]. In these studies it was found that most Rydberg states excited in an electric field and located on the downfield side of the potential are short lived whenever their energy lies above the classically field-induced ionization threshold. On the other hand, Rydberg states that are located on the upfield side of the potential have in general a much longer lifetime. In time-resolved studies of the electron dynamics with short optical pulses, the initial state is still confined to the core region and therefore in general both red and blue states are excited simultaneously [18]. In the case discussed in this paper, where the *initial* state is given by an oriented Rydberg state, the final states will have that same orientation after absorption of the far-infrared photon, enabling the study of completely oriented blue and red Rydberg wave packets in both the frequency and the time domain.

Figure 1 illustrates the principle of the experiments discussed in this paper. Stark states of cesium are shown as a function of the static electric field. Stark states with increasing energy as a function of the field strength have a positive dipole moment and are located on the upfield side of the atomic core (blue states). Stark states with decreasing energy as a function of the field strength are located on the downfield side (red states). The field-induced ionization limit E_c is given by

$$E_c = -6.12\sqrt{F}, \tag{1}$$

where F is the electric field strength in V/cm and E_c is given in cm^{-1} (thick line in Fig. 1). The states marked A (at -456.3 cm^{-1}) and B (at -464.6 cm^{-1}), which are adiabati-

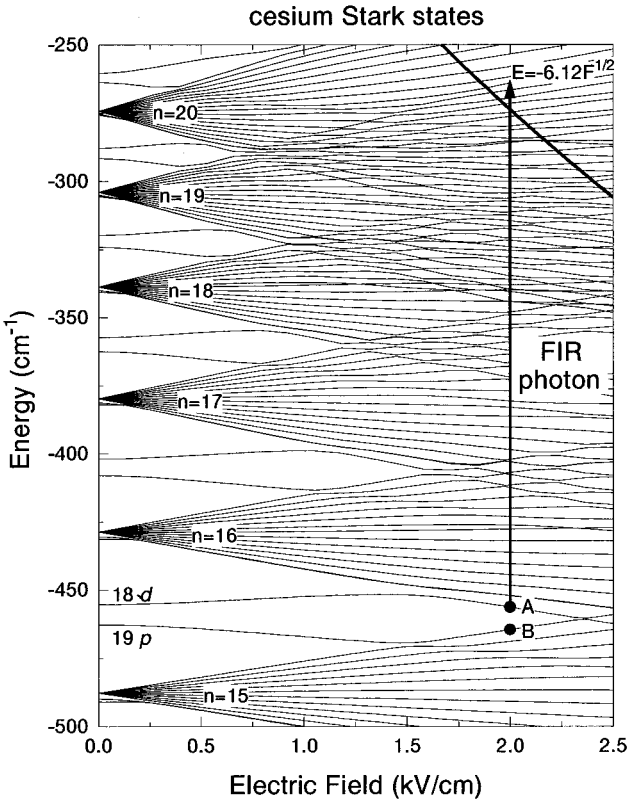

FIG. 1. Energy levels of cesium Stark states as a function of the electric field. At 2.0 kV/cm the two initial states A and B are marked. State A is a red state of which the wave function is dominantly located on the uphill side. State B is a blue state, wave function dominantly located on the downfield side. Also shown (thick line) is the field-induced ionization threshold.

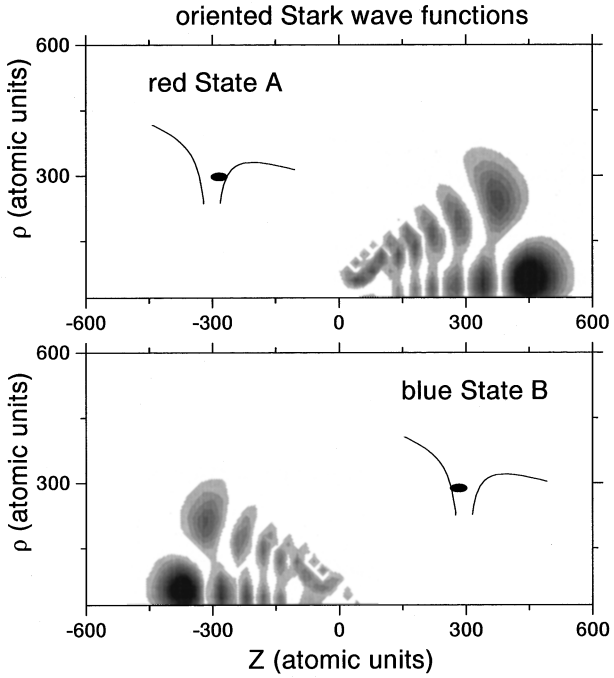

FIG. 2. The upper and lower graphs show contour plots of the wave functions of state A and B in Fig. 1, respectively, as a function of Z (along the direction of the electric field) and ρ (distance to the Z axis). The saddle point in the potential is located at positive Z.

cally connected to the $18d$ and $19p$, respectively, can both be optically excited with a one-photon transition from the $6s$ ground state of cesium, since at 2 kV/cm the p character that is necessary for the one-photon excitation is spread over the Stark states due to their coupling via the electric field. In Fig. 2 the calculated wave functions of both the red and blue states are shown in a contour plot. The calculations are done along the lines of Ref. [19]. The figure shows that the Stark states are indeed strongly oriented with respect to the nucleus (located at $Z=0$).

After preparation of these states, the Rydberg electron can be further excited with the use of a far-infrared photon to a state that lies above the classical field ionization limit. Depending on which initial state is excited (A or B) the wave function of the far-infrared excited Rydberg electron will be dominantly located on the upfield (blue state B) or downfield (red state A) side, respectively. This can be understood in terms of the overlap integrals between the initial and final wave functions, which determines the cross section, and have been calculated explicitly for hydrogen [20].

In this paper we present photoionization spectra, starting from the initial Rydberg states such as A and B in Fig. 1, to the quasicontinuum that lies above the classical field ionization limit. To study this, far-infrared radiation is used with wavelengths ranging from 180 to 1400 cm^{-1}. Furthermore we have studied the time-dependent electron emission of the autoionizing states using an atomic streak camera with picosecond time resolution. Finally we discuss how the observed properties of these Rydberg atoms can be applied in ultrafast far-infrared detectors as well as wavelength-dependent detectors of the far-infrared radiation.

II. EXPERIMENT

A thermal beam of cesium atoms, located in between two plates creating a static electric field 1–4 kV/cm, are excited with a tunable nanosecond dye laser that is pumped by the second harmonic of a Nd:YAG laser operating at 10 Hz. The output of the dye laser ($630-650$ nm) is frequency doubled in a potassium dihydrogen phosphate (KDP) crystal. In this way Rydberg states are excited with energies below the saddle-point energy. After excitation with the dye laser, the atoms are exposed to a picosecond far-infrared pulse with a tunable wavelength ranging from 100–1600 cm^{-1} ($\lambda=6-100$ μm). The far-infrared pulses are generated from a free-electron laser FELIX in Nieuwegein, the Netherlands [21]. This laser generates trains of ~ 5000 micropulses with a temporal spacing of 1 ns at a repetition rate of 5 Hz. The spectral width of the far-infrared pulses can be varied from 0.4% of the photon energy as used for the far-infrared spectra up to 3% for the dynamical studies. The energy per micropulse is in the microJoule regime and can be controlled using broadband attenuators. The micropulses are weakly focused in the interaction region giving a peak power of <10 MW/cm^2. The far-infrared ionization spectra are recorded by integrating the electron yield of the first seven far-infrared pulses after the optical preparation of the initial Rydberg state by the dye laser.

To study the time-dependent electron emission of Rydberg wave packets, an atomic streak camera is used. The

camera is able to measure the electron emission of atoms with picosecond time resolution [22]. In this case only a single far-infrared micropulse is selected. The electrons escaping from the atoms are accelerated in the static electric field and enter the deflection region. Due to the ramped voltage on the deflection plates, the electrons are deflected depending on the time of arrival between the deflection plates. The deflection angle is measured by detecting the position of the electrons after a 20-cm flight path. The creation of the voltage ramp is done with a GaAs photoswitch [22], which is triggered by the second harmonic of a Nd:YAG laser (pulse duration 200 ps), which is synchronized with a micropulse of the free-electron laser (time jitter $\ll 1$ ns). Both electrons appearing from far-infrared pulses before and after the selected micropulse will not reach the detector since at the time of arrival of these electrons between the deflection plates, the voltage will be such that the deflection is too large to reach the detector.

Great care was taken to avoid absorption of part of the far-infrared spectrum by water vapor since these absorptions significantly change the temporal profile of the far-infrared pulses. To avoid this, the far-infrared laser beam was transported through a vacuum tube close to the vacuum chamber. The remaining path (20 cm) was sealed and put at over pressure by a dry nitrogen flow.

III. FAR-INFRARED IONIZATION SPECTRA

In this section we present photoionization spectra of oriented cesium Rydberg states in a static electric field of 2.0 kV/cm. In Fig. 3 the ionization spectra are shown for two cases. In Fig. 3(a) the blue state (B) is the initial Rydberg state and in Fig. 3(b) the red state (A) is the initial state. Even though the energy difference between the initial Rydberg states is small, $\Delta E_{\mathrm{blue,red}}=8.3\ \mathrm{cm}^{-1}$, the measured ionization spectra differ dramatically. For the blue initial state we observe sharp resonances in the cross section, whereas for the red initial state a more continuous spectrum is observed. For the red initial state structure is found only when the far-infrared frequency approaches the field-induced ionization threshold. For a field of 2.0 kV/cm the photoionization threshold is at a photon energy of 183 cm^{-1} ($\lambda=54.7$ μm) for the red state and 191 cm^{-1} ($\lambda=52.4$ μm) for the blue state. The output of the free-electron laser is approximately a factor of 1.5 lower at the highest photon energy compared to the lowest photon energy plotted in Fig. 3. The yield is not corrected for this variation. The bandwidth of the laser is chosen to be 1 cm^{-1}, and the polarization is perpendicular to the static electric field. The dashed line shows a MQDT calculation of the absorption spectrum. Both experiment and theory shows that photoionization of a blue Rydberg states is restricted a few, well-defined, photon energies.

The differences between the blue and red ionization spectra shown in Fig. 3 arise from the different orientations of the initial Rydberg wave function. As mentioned in the Introduction when a blue initial Rydberg state is excited, it is expected that on the basis of the overlapping wave function, after absorption of a far-infrared photon, the final state will also have dominantly blue character. Also plotted in Fig. 3(a) are the extreme blue members of the higher-lying hydrogen

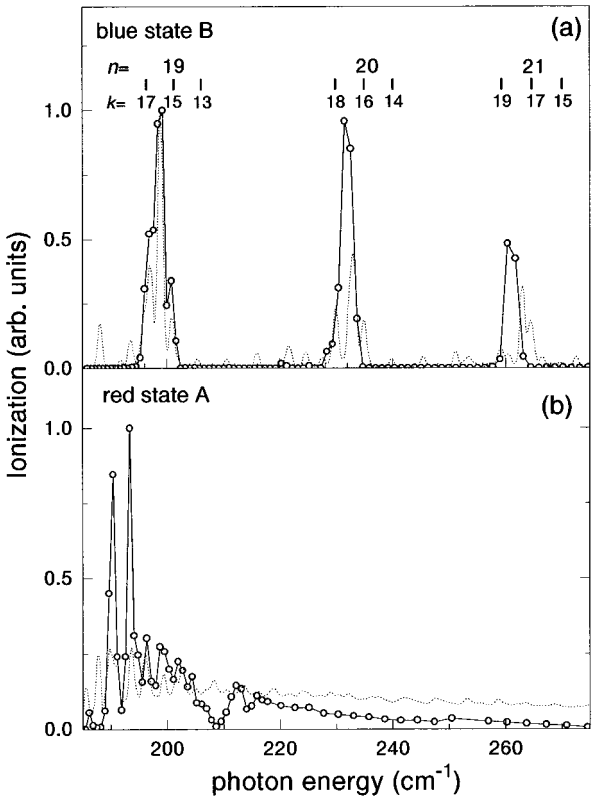

FIG. 3. (a) Photoionization spectrum as a function of excitation energy starting from the blue state, marked A in Fig. 1. Also plotted are the hydrogenic, $m=1$, energy levels of the extreme blue Stark states in this energy regime. (b) Photoionization spectrum starting from red state B, as indicated in Fig. 1. The far-infrared laser polarization is perpendicular to the electric field of 2.0 kV/cm. The dotted curves correspond to the calculation described in the text.

Stark manifolds. It is observed that only the extreme blue members of the manifolds in the quasicontinuum have a substantial ionization cross section. For hydrogen, the strengths of transitions between Rydberg states have been calculated [23]. The hydrogenic matrix elements are non-negligible for transitions where $(n,n_1,n_2,m)\rightarrow(n\pm p,n_1\pm p,n_2,m)$ in the case of $n_1\gg n_2$. n_1,n_2 are the parabolic quantum numbers, defining the Stark state energy as

$$E_{n,n_1,n_2}=\frac{-1}{2n^2}+\frac{3}{2}(n_1-n_2)nF. \tag{2}$$

For the extreme blue state k ($\equiv n_1-n_2$) equals $n-1$ for $m=0$ states ($n-2$ for $m=1$ states) and for the extreme red state k equals $-n+1$ ($-n+2$ for $m=1$). In Fig. 3(a) transition from (15,14,0,0) to (19,17,0,1), (20,18,0,1), and (21,19,0,1) have non-negligible matrix elements for hydrogen. Since hydrogenic energy levels are plotted in Fig. 3 up to second-order perturbation, the slight mismatch between the measured and observed resonances probably stems from the fact that the quantum defects, which are pronounced for cesium, are not taken into account. When the far-infrared laser polarization is chosen parallel to the electric field (not shown) the results are similar: starting from state B photoionization only occurs at the location of blue quasicontinuum states.

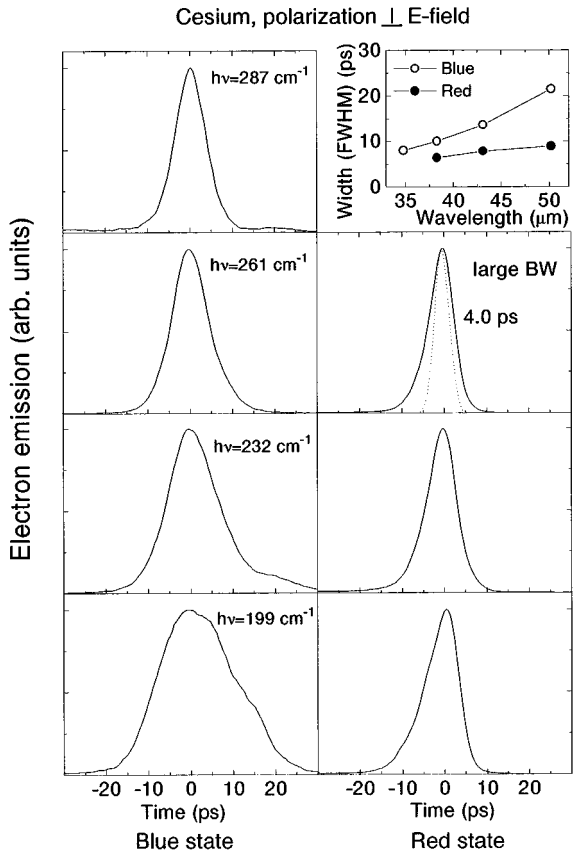

FIG. 4. Time-resolved electron emission transients of cesium Rydberg atoms. The quasicontinuum states are excited from an initial blue Stark state (left column) and an initial red Stark state (right column). The polarization of the far-infrared pulse is chosen perpendicular to the electric field of 2.0 kV/cm. The inset shows the width (FWHM) of the measured photoionization spectra. The dotted line shows the electron emission transient for a larger bandwidth of the far-infrared radiation.

For excitation from the initial *red* Rydberg state A, the spectrum has a more continuous character. The splitting between the states belonging to one Stark manifold as a function of the field is given by $\Delta E_k = 3Fn$. For higher n, the number of Stark states increases as well as the energy splitting between the Stark states belonging to one manifold. Therefore red Stark states from higher n manifolds will have overlap with red Stark states from lower n manifolds. Furthermore, the red states that are excited have a very short lifetime and are therefore broad resonances. Both the presence of many red states within the bandwidth of the far-infrared laser pulse and their short lifetime gives rise to this more continuous ionization spectrum.

IV. TIME-RESOLVED ELECTRON EMISSION

A. Electron emission transients of oriented Rydberg states

With the use of an atomic streak camera the time-resolved electron emission of these Rydberg states A and B is measured after excitation with the far-infrared radiation. In Fig. 4 time-resolved electron emission transients of cesium atoms in a static field of 2.0 kV/cm are shown. In the left column the electron emission transients are shown from the initial blue Stark state B. The far-infrared laser wavelength is tuned to the resonances as shown in Fig. 3(a). In the right column the electron emission transients are shown from the initial state given by the red Stark state (state A in Fig. 1). In both cases the far-infrared radiation is polarized perpendicular to the electric field.

Starting with the left column of Fig. 4 we observe an increase in lifetime of the Rydberg state as we decrease the excitation energy. Approaching from above the field-induced ionization limit, located at a binding energy of -274 cm^{-1}, i.e., at a photon energy of 191 cm^{-1} from the initial blue state B, the lifetime of the Rydberg states increase [24]. In previous experiments where ground-state atoms were excited to the quasicontinuum states it was also found that when dominantly blue states were excited the lifetime increased considerably when the excitation was close to the field-induced ionization limit [4,3,25,18]. Since in those experiments the excitation is from the ground state, both red and blue Stark states can be excited, making it more difficult to excite the pure blue Stark states. Here the initial state is a blue Stark state, and therefore after absorption of the far-infrared photon the wave function will still be located on the upfield side of the potential. The absence of structure in these electron emission transients is given by the fact that only a single state is dominantly excited and therefore there is no interference structure expected in the electron emission.

The right column of Fig. 4 shows the electron-emission transients starting from the red Stark state for the same photon energies of the far-infrared radiation as in the left column of Fig. 4. Since after absorption of the far-infrared photon the energy of the electron is above the field-induced ionization threshold, E_c, and the wave function is located on the downfield side near the saddle point in the potential, we observe that the ionization is prompt, i.e., faster than the optical pulse duration given by 5 ps. The slight difference in energy between the initial blue and red Stark states (8.3 cm^{-1}) did not change the transients of the red ionizing states and is therefore neglected. The dotted line in the right column of Fig. 4 shows the electron emission transients when a larger bandwidth of the far-infrared radiation is selected, i.e., a shorter pulse duration. The temporal width of the measured electron emission transient narrows down to 4 ps [full width at half maximum (FWHM)] showing that the temporal width of the other electron emission traces are limited by the pulse duration of the far-infrared laser pulse, rather than the time resolution of the streak camera.

In Fig. 5 the calculated electron probablity distribution of the ionizing wave packet is plotted starting from the red state A. Unlike the bound wave functions plotted in Fig. 2 an outgoing electron flux to positive Z is clearly observed. The distribution is plotted at $\tau = 0$, i.e., at the peak of the far-infrared laser pulse of 5 ps (FWHM).

B. Comparison between optical and far-infrared excited wave packets

In the optical regime, the decay of autoionizing wave packets in electric fields has been studied before with the atomic streak camera [18]. In those experiments, Rydberg wave packets were excited from the ground state of the atom in a one-photon transition. The ionization dynamics was ex-

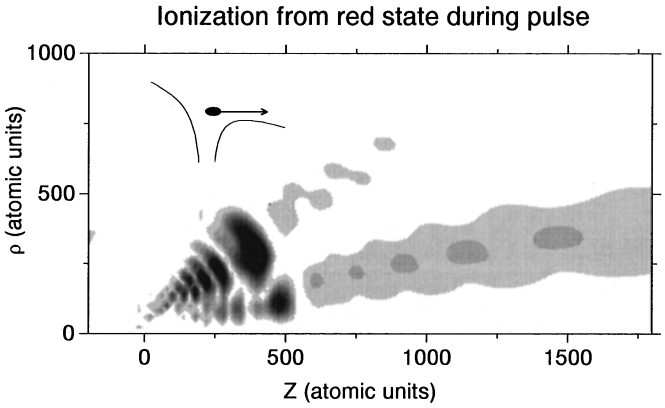

FIG. 5. Contour plot of the electron probability distribution of a wave packet excited from the red initial state with far-infrared radiation of 261 cm^{-1}. The distribution is shown at $\tau=0$, i.e., the far-infrared pulse is then at its peak value. The outgoing electron flux is clearly observed by the probability at large Z. The dotted lines show the calculated electron flux. Just above the saddle-point energy, at 0.94 E_c, the theory is unable to match the measured flux.

plained in terms of core scattering of the Rydberg electron whenever it came into a low l state, since the point of nearest approach to the core is given by $r_{\min}\sim l(l+1)$. This behavior was observed in the pronounced oscillatory electron emission, where the spacing between the electron emission bursts was given by the angular momentum oscillation time of the excited wave packet. In those experiments, the excitation was done from the ground state of the atom, and therefore the initial state was confined to the core region. With the use of far-infrared radiation, the ionization dynamics is now studied by starting from a Rydberg state. In Fig. 6 time-resolved electron emission transients are shown by cesium Rydberg wave packets excited from the initial red Rydberg state (left column) and the 6s ground state (right column). The excitation is to -195 cm^{-1}, -225 cm^{-1}, and -258 cm^{-1} ($0.71E_c$, $0.82E_c$, and $0.94E_c$) and perpendicular to the electric field of 2.0 kV/cm for both cases. Along the lines of Ref. [19] the electron emission transients are calculated (dotted lines of Fig. 6). The spectral width of the far-infrared pulse (left column) is given by ~ 3 cm^{-1}, whereas for the optical pulse (right column) the bandwidth is given by 14 cm^{-1} (FWHM). For the excitation from the red Stark state no structure is observed, whereas the ground-state excitation shows pronounced oscillations in the electron emission transients. At -258 cm^{-1} ($0.94E_c$) the red state ionization is still very fast whereas the ground-state ionization occurs on a 50-ps time scale. Comparing these transients clearly shows the differences in excited states. At the same final-state energy, different coherent wave packets of angular momentum states, $\Sigma a_l e^{i\Phi_l}|l\rangle$ are excited, both in amplitude a_l and phase Φ_l. This gives rise to the different ionization behavior of the excited wave packets.

V. APPLICATIONS OF ORIENTED RYDBERG ATOMS AS FAR-INFRARED DETECTORS

A. Rydberg atoms as ultrafast far-infrared detector

The use of Rydberg atoms as far-infrared detectors was suggested in 1976 by Kleppner and Ducas [8,26,27]. Due to

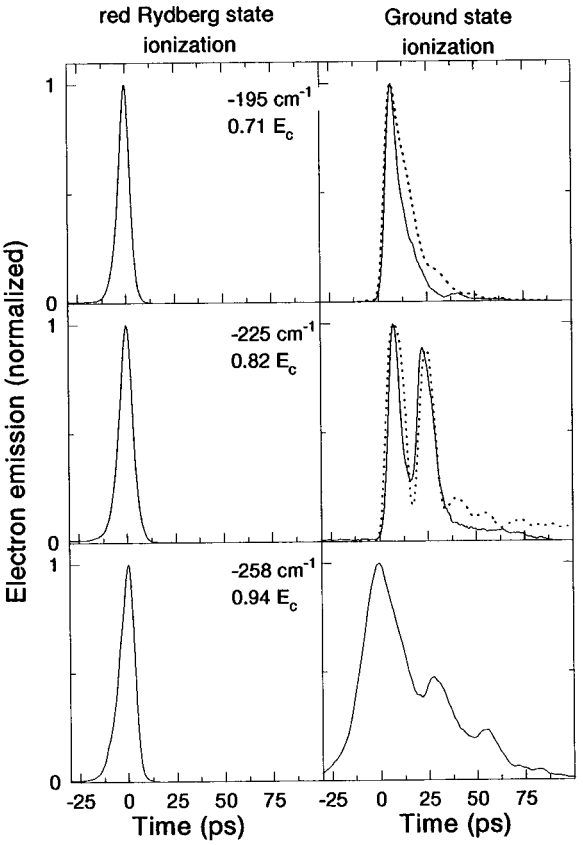

FIG. 6. Time-resolved electron emission transients of cesium Rydberg atoms. The left column shows the transients of ionizing wave packets excited from the initial red Rydberg state with far-infrared radiation. The right column shows the transients of ionizing wave packets excited from the ground state (6s) of cesium with optical radiation around 320 nm to the same energy as the states excited in the left column. The polarization of the laser is perpendicular to the electric field of 2.0 kV/cm in both cases. The dotted curves correspond to the calculation described in the text.

the large overlap between initial and final state, Rydberg atoms have a large far-infrared ionization cross section [28]. In an experiment by Ducas *et al.* [8] it was shown that bound-bound transitions between Rydberg states by far-infrared radiation, followed by state-selective field ionization, enabled them to detect far-infrared radiation with large wavelength selectivity (bandwidth 1 MHz). From our observations discussed in Sec. IV we conclude that when the red initial state is chosen the large ionization cross section is combined with a fast ejection of the electron. For the shortest pulses available from the free-electron laser, we observed time-resolved electron emission transients with a temporal width of 1.2 ps (FWHM) at a photon energy of 286 cm^{-1} ($\lambda=35$ μm). The measured width is very close to the expected width of the far-infrared laser pulses, and therefore the conclusion can be drawn that a far-infrared streak camera, using these red Rydberg states as far-infrared detector has a resolution of approximately 1 ps. A far-infrared streak camera based on Rydberg atoms is discussed in detail elsewhere [29–31].

B. Rydberg atoms as wavelength selective detector

As shown in Fig. 3(a) the photoionization cross section of the cesium blue Rydberg state shows a large selectivity in

wavelength. Ionization occurs at specific wavelengths in the far-infrared regime. We observe that only ionization to extreme blue states possesses a significant cross section. Therefore, by changing the static electric field or choosing a different initial Stark state, the wavelength at which photoionization takes place can easily be controlled. A far-infrared detector based on blue Rydberg atoms will be sensitive for the selected wavelength rather than for the broadband blackbody radiation. Even though these blue states have a longer lifetime than the fast ionizing red states, they can still be considered as fast (<100 ps) far-infrared detectors, with the addition of a strong wavelength selectivity.

VI. CONCLUSIONS

We have studied transitions from bound Rydberg states to quasicontinuum states in a static electric field using a far-infrared laser, in both the frequency and the time domain. For initial Rydberg wave functions located at the downfield side of the nucleus, the far-infrared photoionization spectra are smooth, and the electron emission occurs on a picosecond time scale. For initial Rydberg wave functions located on the upfield side of the nucleus, the far-infrared photoionization spectra show sharp resonances that can be explained in terms of excitation of extreme blue Stark states of different n manifolds. The lifetime of the wave packets excited from these blue initial Rydberg states is considerably longer than the red wave packets. Comparing the electron emission dynamics starting from the ground state with excitations from a bound Rydberg state shows that different quasicontinuum states are excited at the same final-state energy. However, in both cases the angular motion of the wave packet is reflected in the electron emission, appearing in electron bursts separated by the angular oscillation time of the wave packets. Rydberg atoms can be used as ultrafast far-infrared detectors by choosing the initial Rydberg state on the downfield side of the nucleus. For initial Rydberg states located on the upfield side, a wavelength selective detector can be constructed, where the wavelength selectivity can be controlled with the static electric field and the choice of initial state.

ACKNOWLEDGMENTS

We gratefully acknowledge the skillful assistance of the FELIX staff, in particular Dr. A. F. G. van der Meer. This work is part of the research program of the Stichting Fundamenteel Onderzoek van de Materie (FOM) and was financially supported by the Nederlandse Organisatie voor Wetenschappelijk Onderzoek (NWO).

[1] R. R. Freeman, N. P. Economou, G. C. Bjorklund, and K. T. Lu, Phys. Rev. Lett. **41**, 1463 (1978).
[2] M. G. Littman, M. M. Kash, and D. Kleppner, Phys. Rev. Lett. **41**, 103 (1978).
[3] B. Broers, J. F. Christian, and H. B. van Linden van den Heuvell, Phys. Rev. A **49**, 2498 (1994).
[4] B. Broers, J. F. Christian, J. H. Hoogenraad, W. J. van der Zande, H. B. van Linden van den Heuvell, and L. D. Noordam, Phys. Rev. Lett. **71**, 344 (1993).
[5] A. ten Wolde, L. D. Noordam, A. Lagendijk, and H. B. van Linden van den Heuvell, Phys. Rev. A **40**, 485 (1989).
[6] J. A. Yeazell and C. R. Stroud, Jr., Phys. Rev. A **43**, 5153 (1991).
[7] R. R. Jones and P. H. Bucksbaum, Phys. Rev. Lett. **67**, 3215 (1991).
[8] T. W. Ducas, W. P. Spencer, A. G. Vaidyanathan, W. H. Hamilton, and D. Kleppner, Appl. Phys. Lett. **35**, 382 (1979).
[9] E. J. Galvez, C. W. MacGregor, B. Chaudhuri, S. Gupta, E. Massoni, and F. DeZela, Phys. Rev. A **55**, 3002 (1997).
[10] N. E. Tielking and R. R. Jones, Phys. Rev. A **52**, 1371 (1995).
[11] R. B. Vrijen, G. M. Lankhuijzen, and L. D. Noordam, Phys. Rev. Lett. **79**, 617 (1997).
[12] J. H. M. Neijzen and A. Dönszelmann, J. Phys. B **15**, L87 (1982).
[13] P. M. Koch and D. R. Mariani, Phys. Rev. Lett. **46**, 1275 (1981).
[14] J. Y. Liu, P. McNicholl, D. A. Harmin, I. Ivri, T. Bergeman, and H. J. Metcalf, Phys. Rev. Lett. **55**, 189 (1985).
[15] M. G. Littman, M. L. Zimmerman, and D. Kleppner, Phys. Rev. Lett. **37**, 486 (1976).
[16] E. Luc-Koenig and A. Bachelier, J. Phys. B **13**, 1743 (1980).
[17] R. Damburg and V. Kolosov, J. Phys. B **9**, 3149 (1976).
[18] G. M. Lankhuijzen and L. D. Noordam, Phys. Rev. Lett. **76**, 1784 (1996).
[19] F. Robicheaux and J. Shaw, Phys. Rev. Lett. **77**, 4154 (1996).
[20] H. Bethe and E. Salpeter, *Quantum Mechanics of One- and Two-Electron Atoms* (Springer, Berlin, 1957).
[21] D. Oepts, A. F. G. van der Meer, and P. W. van Amersfoort, Infrared Phys. Technol. **36**, 297 (1995).
[22] G. M. Lankhuijzen and L. D. Noordam, Opt. Commun. **129**, 361 (1996).
[23] M. Bellermann, T. Bergeman, A. Haffmans, P. M. Koch, and L. Sirko, Phys. Rev. A **46**, 5836 (1992).
[24] T. F. Gallagher, *Rydberg Atoms*, 1st ed. (Cambridge University Press, Cambridge, 1994).
[25] G. M. Lankhuijzen and L. D. Noordam, Phys. Rev. A **52**, 2016 (1995).
[26] H. Figger, G. Leuchs, R. Straubinger, and H. Walther, Opt. Commun. **33**, 37 (1980).
[27] D. Kleppner and T. W. Ducas, Bull. Am. Phys. Soc. **21**, 600 (1976).
[28] J. H. Hoogenraad and L. D. Noordam (unpublished).
[29] G. M. Lankhuijzen and L. D. Noordam, Nucl. Instrum. Methods Phys. Res. B **375**, 651 (1996).
[30] M. Drabbels and L. D. Noordam, Opt. Lett. **22**, 1436 (1997).
[31] M. Drabbels, G. M. Lankhuijzen, and L. D. Noordam (unpublished).